Acupuncture and Herbal Medicine

Map activation of various brain regions using different frequencies of electroacupuncture ST36, utilizing the FosCreER strategy

Zi Guo[1,2,3], Naixuan Wei[1,2,3], Ru Ye[1,2,3], Tiancheng Sun[4], Shuang Qiu[4], Xiaomei Shao[1,2,3], Xiaochang Ge[1,2,3], Lu Guan[1,2,3], Junfan Fang[1,2,3,*], Jianqiao Fang[1,2,3,*], Junying Du[1,2,3,*]

[1]Department of Neurobiology and Acupuncture Research, The Third School of Clinical Medicine, Zhejiang Chinese Medical University, Hangzhou, China; [2]Key Laboratory of Acupuncture and Neurology of Zhejiang Province, Zhejiang Chinese Medical University, Hangzhou, China; [3]Key Laboratory for Research of Acupuncture Treatment and Transformation of Emotional Diseases, Zhejiang Chinese Medical University, Hangzhou, China; [4]Departments of Neurobiology and Anesthesiology of Second Affiliated Hospital, Zhejiang University School of Medicine, Hangzhou, China

Abstract

Objective: Electroacupuncture (EA) is an alternative treatment option for pain. Different frequencies of EA have different pain-relieving effects; however, the central mechanism is still not well understood.

Methods: The Fos2A-iCreER (TRAP):Ai9 mice were divided into three groups (sham, 2 Hz, and 100 Hz). The mice were intraperitoneally injected with 4-hydroxytamoxifen (4-OHT) immediately after EA at Zusanli (ST36) for 30 min to record the activated neurons. One week later, the mice were sacrificed, and the number of TRAP-treated neurons activated by EA in the thalamus, amygdala, cortex, and hypothalamus was determined.

Results: In the cortex, 2 Hz EA activated more TRAP-treated neurons than 100 Hz EA did in the cingulate cortex area 1 (Cg1) and primary somatosensory cortex (S1), and 2 and 100 Hz EAs did not differ from sham EA. TRAP-treated neurons activated by 2 Hz EA were upregulated in the insular cortex (IC) and secondary somatosensory cortex (S2) compared with those activated by 100 Hz and sham EA. In the thalamus, the number of TRAP-treated neurons activated by 2 Hz EA was elevated in the paraventricular thalamic nucleus (PV) compared with those activated by sham EA. In the ventrolateral thalamic nucleus (VL), the number of TRAP-treated neurons activated by 2 Hz EA was significantly upregulated compared with those activated by 100 Hz EA, and sham EA showed no difference compared with 2 or 100 Hz EA. TRAP-treated neurons were more frequently activated in the ventral posterolateral thalamic nucleus (VPL) by 2 Hz EA than by 100 Hz or sham EA.

Conclusions: Low-frequency EA ST36 effectively activates neurons in the Cg1, S1, S2, IC, VPL, PV, and VL. The enhanced excitability of the aforementioned nuclei induced by low-frequency EA may be related to its superior efficacy in the treatment of neuropathological pain.

Keywords: Amygdala, Cortex, EA-TRAPed neurons, Electroacupuncture, Frequency, Hypothalamus, Thalamus

Graphical abstract: http://links.lww.com/AHM/A104.

Introduction

Acupuncture is a traditional Chinese therapy[1] which is highly effective for treating various pain conditions, with negligible side effects[2–5]. It is now used as an alternative treatment for many diseases[6–10]. Acupuncture therapy involves manual acupuncture and electroacupuncture (EA), which combines traditional manual acupuncture with modern electrical technology. The effectiveness of EA depends on the acupoint chosen, frequency, and other factors[11–13]. Zusanli (ST36) is an acupoint on the Foot-Yangiming Meridian[14,15], also known as the Xiahe point, which plays an effective role in treating pain[16–18]. Studies have demonstrated that EA at the ST36 acupoint causes a noticeable increase in c-Fos expression in the central nervous system[19] compared with non-acupoint EA. It is also crucial to note that the effectiveness of EA is significantly affected by frequency[20,21]. The effectiveness of different EA frequencies for pain relief varies. EA at 2 Hz is more effective for treating neuropathic pain[22], whereas

*Corresponding author. Jianqiao Fang, E-mail: fangjianqiao7532@163.com; Junfan Fang, E-mail: fangjunfan0223@163.com; Junying Du, E-mail: dujunying0706@163.com.

Received 17 October 2023 / Accepted 25 February 2024

How to cite this article: Guo Z, Wei NX, Ye R, Sun TC, Qiu S, Shao XM, Ge XC, Guan L, Fang JF, Fang JJ, Du JY. Map activation of various brain regions using different frequencies of electroacupuncture ST36, utilizing the Fos-CreER strategy. Acupunct Herb Med 2024;4(3):386–398. DOI: 10.1097/HM9.0000000000000106

100 Hz EA is commonly used to alleviate inflammatory pain[23,24]. Previous studies have reported that EA modulates the excitability of neurons in brain areas such as the cortex and amygdala, including the cingulate cortex area 1 (Cg1), prelimbic cortex (PrL), primary somatosensory cortex (S1), and central amygdaloid nucleus (CeA)[25,26]. However, the direct regulation of neurons by EA and whether different EA frequencies have similar effects on the regulation of brain areas remain uncertain.

The potential mechanism of EA-induced analgesia has received extensive attention over the years, and many studies have demonstrated that EA relieves pain by modulating specific neuronal populations, signaling pathways, or various substances in the brain[27–29]. For instance, endogenous cannabinoid receptor 1 (CB1Rs) is activated by EA and has analgesic effects by inhibiting GABAergic neurons and activating glutamatergic neurons in the ventrolateral periaqueductal gray (vlPAG)[30]; EA reduces p-ERK expression in the right hindlimb S1 and bilateral Cg1 to relieve inflammatory pain[31]. Although the preliminary observations using immunofluorescence or western blotting techniques suggest that EA relieves pain by modulating substances or neurons in different brain regions that are activated. It is still unknown whether EA directly modulates the "activity" neurons to relieve pain.

Immediate early genes (IEGs) constitute the most extensively investigated approach for elucidating the connection between gene expression and neuronal activity[32,33], which defines their response properties[34,35]. Fos, as an IEG[36], is a generic indicator of neuronal activity that is quickly and momentarily triggered by external stimuli[37,38] Many methods have been exploited to identify activity-dependent Fos expression, such as intracellular calcium imaging; however, they have several drawbacks, including a low signal-to-noise ratio, transience of effector protein expression, and poor temporal resolution[39].

The FosCreER system, which expresses activity-dependent Fos when CreERT2 recombines in the presence of Tamoxifen[24], visualizes and manipulates activated neurons within a limited time window. This method labels the activated neurons more precisely and reliably. Recently, Guo et al. reported the use of this method to record activated neurons in different brain regions using manual acupuncture Neiguan (PC6) acupoint[24]. Therefore, we believe that the FosCreER system can be applied to the experiments, regardless of whether EA ST36 directly modulates the "activity" neurons.

In this study, Fos-iCreERT2:Ai9 double transgenic mice were specifically labeled with TRAP-treated neurons at 2 or 100 Hz to map the activation of various brain regions and investigate the EA ST36's neural network mechanism at various frequencies. Different brain areas may be differently activated during high- and low-frequency EA treatments. This variation in brain activation may be linked to specific therapeutic indications.

Materials and methods

Animals

Male Fos2A-iCreER (TRAP) mice (Stock No: 030323) and Ai9 mice (Stock No: 007909) were obtained from Jackson Laboratory. FosTRAP:Ai9 mice (age range: 8–15 weeks old; weight range: 18–22 g), obtained from a cross between FosTRAP and Ai9 mice, were utilized in this study. The mice were raised at the Experimental Animal Center of Zhejiang Chinese Medical University under carefully controlled circumstances, including a temperature of 25°C and a 12-hour light/dark cycle. They had free access to food and water. Each experiment was conducted daily between 9:00 and 17:00. All experimental protocols were approved by the Zhejiang Chinese Medical Animal Care and Welfare Committee of Zhejiang, China (IACUC-20200302-06). They were maintained in a single cage to avoid interference from other external factors.

Drug preparation

A 20 mg/mL solution of 4-hydroxytamoxifen (4-OHT, Shanghai Yuanye Bio-Technology Co., Ltd., S80892) in ethanol was prepared by shaking at 37°C for 15 min. Corn oil (Shanghai Yuanye Bio-Technology Co., Ltd., S50856) was added to the solution, the final concentration of 4-OHT was 10 mg/mL, and the ethanol was evaporated by vacuum under centrifugation. Subsequently, 50 mg/kg 4-OHT was delivered through intraperitoneal (i.p.) injection.

Target recombination in active population of EA intervention

The FosTRAP:Ai9 mice were randomly assigned to the following groups: 2 Hz EA, 100 Hz EA, and sham EA. ST36 is one of the main acupoints of the Foot-Yangiming meridian, known as the Xiahe point. A great deal of practice has confirmed that ST36 is an important acupuncture point for preventing and curing many diseases and strengthening the body[40]. We have previously found that EA ST36 has a positive effect on inflammatory and neuropathic pain in mice[33,41].

Hz EA TRAP (2 Hz-TRAP)

For FosTRAP 2 Hz EA, mice were attached to an EA-assisted tube, but not subjected to EA, for at least 7 days to adapt to the environment. On the eighth day, we initiated EA stimulation in mice. Acupuncture needles (0.16 mm × 7 mm) were inserted into the bilateral ST36 to a depth of 5 mm and BL60 to a depth of 3 mm. The Hans Acupoint Nerve Stimulator (HANS-200E; Huatuo Co., Ltd., Beijing, China) output terminals were attached to the two ipsilateral needles. The stimulator's parameters were as follows: 2 Hz, 0.3 to 0.5 mA (initial strength 0.3 mA, increased by 0.1 mA every 10 min) for a total of 30 minutes[42,43]. Needles were inserted subcutaneously into ST36 and BL60 in the sham EA group. The needles were connected to the electrodes without electrical stimulation. Mice were i.p. injected with 4-OHT immediately after EA (Figure 1A, B) and no other activities that disturbed the mice, such as feeding and cleaning, were performed for 6 h before or after 4-OHT injection.

100 Hz EA TRAP (100Hz-TRAP)

The stimulator's parameters were as follows: 2 Hz, 0.3 to 0.5 mA (initial strength 0.3 mA, increased by 0.1 mA

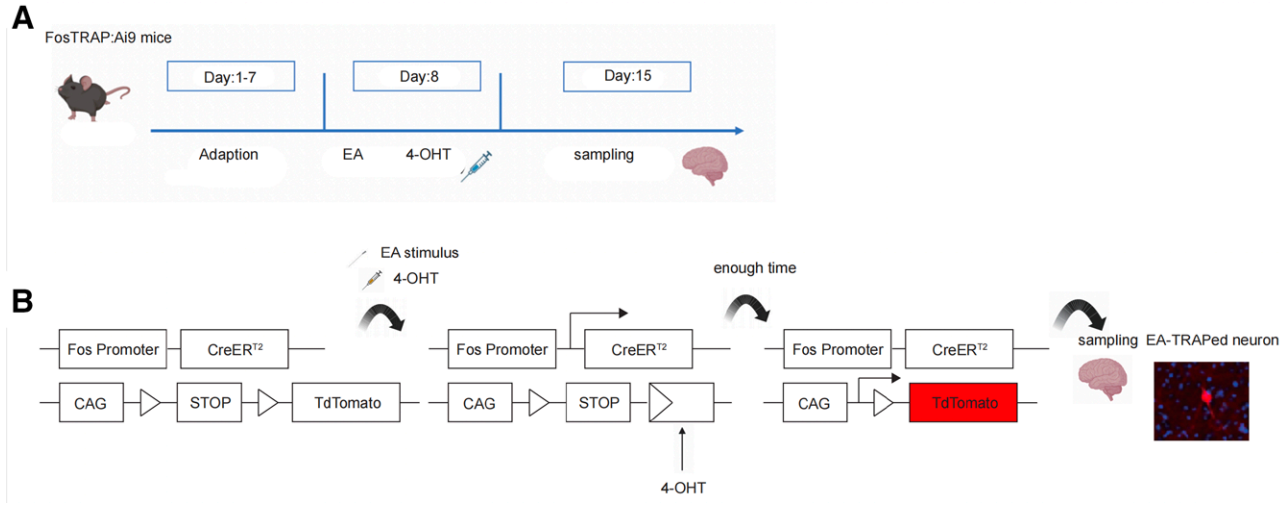

Figure 1. EA directly activates cells in the mouse brain. (A) Timeline of experimental procedures. (B) Intersectional genetic targeting, TRAPed cells activated during EA tagging. 4-OHT: 4-Hydroxytamoxifen; EA: Electroacupuncture.

every 10 min) for a total of 30 min. The other operations were the same as those for the 2 Hz-TRAP.

Sham EA TRAP (sham-TRAP)

Needles were inserted into ST36 and auxiliary points of the animals in the sham EA group. The needles were connected to the electrodes without electrical stimulation.

Histology

After receiving 4-OHT, the mice were kept for 7 days so that enough Fos-positive neurons in the brain could express tdTomato after EA or sham EA treatment. Transcardial perfusion was performed using phosphate-buffered saline (PBS; pH 7.4), followed by 4% paraformaldehyde in PBS. Brain tissues were harvested and stored overnight in 4% paraformaldehyde before being transferred to 15% and 30% sucrose for dehydration. The tissues were embedded in Tissue-Tek O.C.T compound (SAKURA, CA, USA). The brains were sliced into 30 μm sections. Brain sections were mounted on microscope slides in PBS. A water bath-slide dryer (CANY, Jinhua, China) was used to allow the slides to dry for an hour. The sections were then incubated with diamidino-phenyl-indole (Abcam, Cambridge, UK). Brain sections were scanned and examined using the 20× objective of a virtual slide microscope (Olympus, Tokyo, Japan), which is a solitary red stain (tdTomato). Slice images were overlaid on The Mouse Brain in Stereotaxic Coordinates (Keith B. J. Franklin, 2001) to verify the identity of several brain areas. The number of images per square millimeter in each region were counted, and five images from each region were averaged per mouse, resulting in an average of 3 to 5 mice per group.

Statistical analyses

The data were examined using GraphPad Prism 9.4.1 (GraphPad Software, CA, USA) and are shown as the mean ± standard error of the mean. One-way analysis of variance (ANOVA) was used to compare data from various groups, followed by the Tukey *post hoc* test, and values of $P < 0.05$ were utilized as the threshold for determining statistical significance when comparing two groups.

Results

Thalamic nuclei are activated by EA at various frequencies

In the thalamus, we counted the numbers of TRAPed neurons of the sham EA, 2 Hz, and 100 Hz groups in the following nuclei: paraventricular thalamic nucleus (PV), ventrolateral thalamic nucleus (VL), ventral posterolateral thalamic nucleus (VPL), ventral posteromedial thalamic nucleus (VPM), lateral posterior thalamic nucleus (LP), lateral habenular nucleus (LHb), anteroventral thalamic nucleus (AV), laterodorsal thalamic nucleus (LD), mediodorsal thalamic nucleus (MD), posterior thalamic nuclear group (Po), and ventromedial hypothalamic nucleus (VM).

In bilateral VPM, LP, LHb, AV, LD, MD, Po, and VM, the number of TRAPed neurons was not significantly different between the sham, 2 Hz, and 100 Hz groups. The measurements were taken at different coordinates along the bregma axis ranging from –1.06 to –2.54, –1.46 to –3.08, –0.94 to –2.18, –0.34 to –1.22, –0.82 to –1.70, –0.58 to –2.06, –1.34 to –2.70, –0.94 to –2.18 for VPM, LP, LHb, AV, LD, MD, Po, and VM, respectively [Supplementary Figures S1–S4, http://links.lww.com/AHM/A105].

The PV spans from bregma –0.22 to –2.3. In the PV, a notable increase in the number of TRAPed neurons was observed in the 2 Hz group (191.6 ± 24.7%) compared with the sham group (95.92 ± 17.00%); however, no discernible differences were observed between the 100 and 2 Hz group or sham group (Figure 2A–C).

The VL spans from bregma –0.94 to –1.70. On the right VL, the 2 Hz group (21.15 ± 1.497%) had considerably more TRAPed neurons than that of the 100 Hz group (8.00 ± 2.082%); however, the 2 and 100 Hz EA groups exhibited no difference from the sham EA group. On the left side, no discernible difference was observed among the three groups (Figure 2D–F).

The VPL spans from bregma –0.82 to –2.30. At the right VPL, the number of TRAPed neurons in the 2 Hz

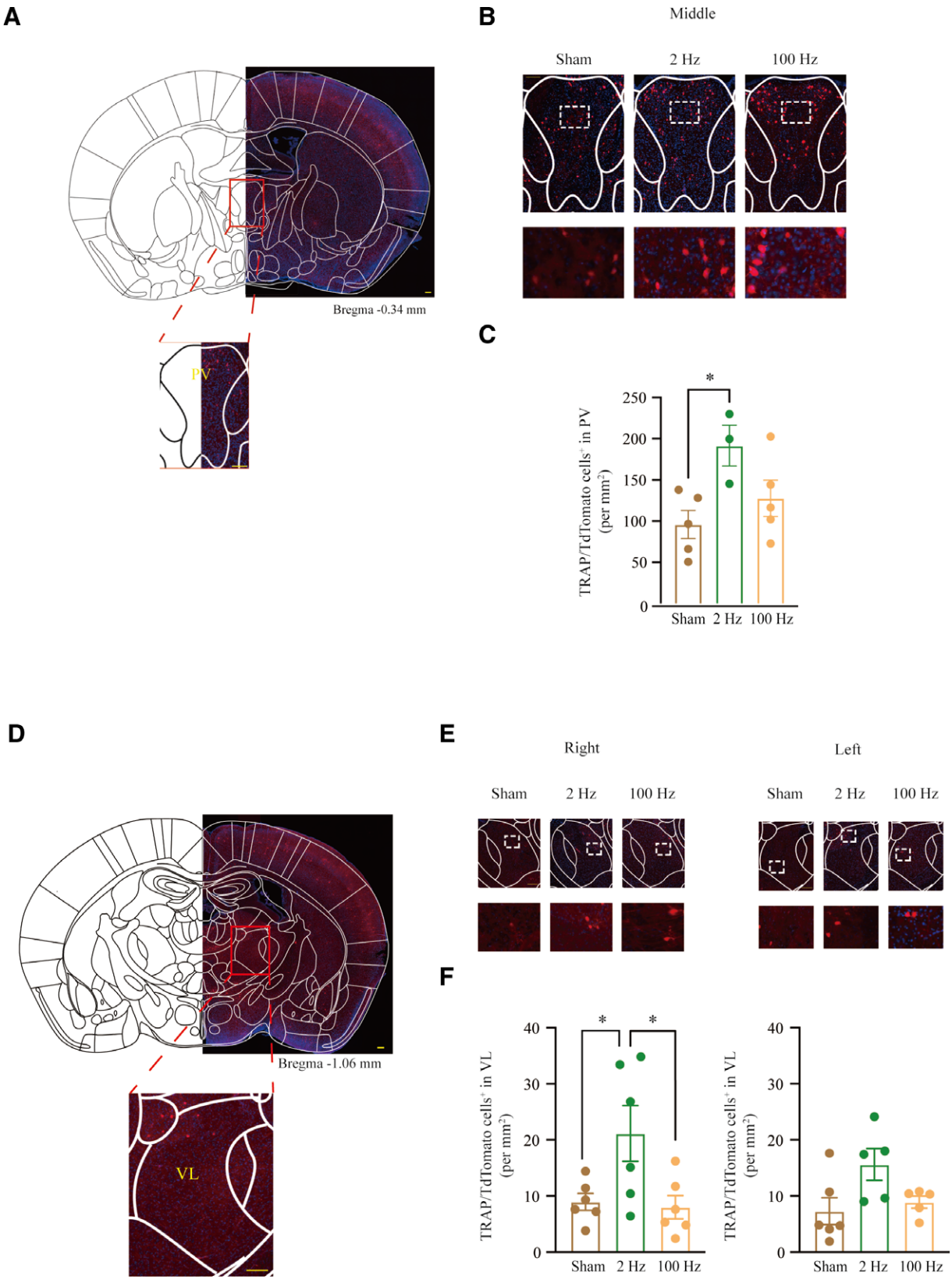

Figure 2. Higher activation of PV VL in the thalamus by 2 Hz EA. (A) A representative figure showing the location of PV. (B) Representative images of EA-TRAPed cells in the bilateral PV in the different groups of mice, the scare bar: 200 μm. (C) In the PV, the number of TRAPed cells activated by EA at 2 Hz was significantly higher than at 100 Hz, data are presented as mean ± SEM, $F_{2,10} = 4.506$, $P = 0.0403$, *post hoc* Tukey test: $P = 0.1623$ (2 *vs*. 100 Hz), $^*P = 0.0328$ (sham *vs.* 2 Hz), $P = 0.5068$ (sham *vs*. 100 Hz), $n = 3$–5. (D) A representative figure showing the location of VL. (E) Representative images of EA-TRAPed cells in the bilateral VL in the different groups of mice, the scare bar: 200 μm. (F) In the VL, the number of TRAPed cells activated by EA at 2 Hz on the right side was significantly higher than at 100 Hz, on the right, data are presented as mean ± SEM, $F_{2,15} = 5.175$, $P = 0.0195$, *post hoc* Tukey test: $^*P = 0.0288$ (2 *vs*. 100 Hz), $^*P = 0.0431$ (sham *vs*. 2 Hz), $P = 0.9764$ (sham *vs* 100 Hz); on the left, $F_{2,13} = 3.768$, $P = 0.0512$, *post hoc* Tukey test: $P = 0.1438$ (2 *vs*. 100 Hz), $P = 0.0505$ (sham *vs*. 2 Hz), $P = 0.8663$ (sham *vs*. 100 Hz), $n = 5$–6, $^*P < 0.05$, compared with 2 Hz. EA: Electroacupuncture; PV: Paraventricular thalamic nucleus; SEM: Standard error of the mean; VL: Ventrolateral thalamic nucleus.

group (10.82 ± 1.426%) increased compared with that of the sham (5.9 ± 0.7714%) and 100 Hz (3.58 ± 0.8345%) group; however, no discernible difference was observed among the three groups at the left VPL (Figure 3A–C).

Cortex nuclei are activated by EA at various frequencies

Seven brain regions were examined: the primary somatosensory cortex (S1), secondary somatosensory cortex (S2), insular cortex (IC), cingulate cortex area 1 (Cg1), cingulate cortex area 2 (Cg2), PrL, and infralimbic cortex (IL).

No significant difference in the number of the TRAPed neurons was observed among the sham, 2 Hz, and 100 Hz groups in bilateral Cg2, PrL, and IL, which spans from bregma 1.42 to –0.22, 3.08 to 1.54, and 1.98 to 1.34, respectively [Supplementary Figures S5–S6, http://links.lww.com/AHM/A106].

The Cg1 spans from bregma 2.34 to –0.22 in the left Cg1, and the TRAPed neurons (41.30 ± 3.859%) in the 2 Hz group were significantly higher than those of the 100 Hz groups (21.22 ± 7.045%); the sham EA group did not differ from the other two groups in any way. However, in the right Cg1, no discernible difference was observed among the three groups (Figure 4A–C).

The S1 spans from bregma 1.98 to –2.30. In the left S1, the number of TRAPed neurons in 2 Hz (111.9 ± 13.21%) group was substantially larger than that of 100 Hz (71.85 ± 10.97%) group; the sham EA group did not differ from the other two groups. However, in the right S1, the three groups did not differ significantly (Figure 4D–F).

The S2 spans from bregma 0.98 to –1.82. The number of 2 Hz TRAPed neurons (61.14 ± 8.349%) increased significantly compared with that of the sham group (33.44 ± 3.149%) and 100 Hz (31.46 ± 4.678%) groups in the right S2; however, in the left S2, no difference was observed among the three groups (Figure 5A–C).

The IC spans from bregma 2.46 to –1.22. In the bilateral IC, 2 Hz EA (left, 81.08 ± 13.92%, right, 74.44 ± 6.428%) activated more TRAPed neurons than the sham (left, 36.80 ± 8.865%, right, 35.62 ± 5.656%) and 100 Hz (left, 41.44 ± 2.188%, right, 42,18 ± 5.969%) groups did (Figure 5D–F).

Activation of amygdala nuclei by EA at different frequencies

We examined seven nuclei below the amygdala, including the posterolateral cortical amygdaloid nucleus (PLCo), basomedial amygdaloid nucleus (BM), basolateral amygdaloid nucleus (BLA), medial amygdaloid nucleus (Me), lateral amygdaloid nucleus (La), posteromedial cortical amygdaloid nucleus (PMCo), and CeA.

Bilateral PLCo, BM, BLA, Me, La, PMCo, and CeA showed no appreciable variation in the number of TRAPed neurons between the sham, 2 Hz, and 100 Hz groups. The measurements were taken at different coordinates along the bregma axis ranging from –1.22 to –2.54, –0.58 to –2.54, –0.58 to –2.06, –0.70 to –2.18, –0.70 to –2.30, –1.82 to –3.80, –0.58 to –1.94, respectively [Figure 6A–F, Supplementary Figures S7–S9, http://links.lww.com/AHM/A107].

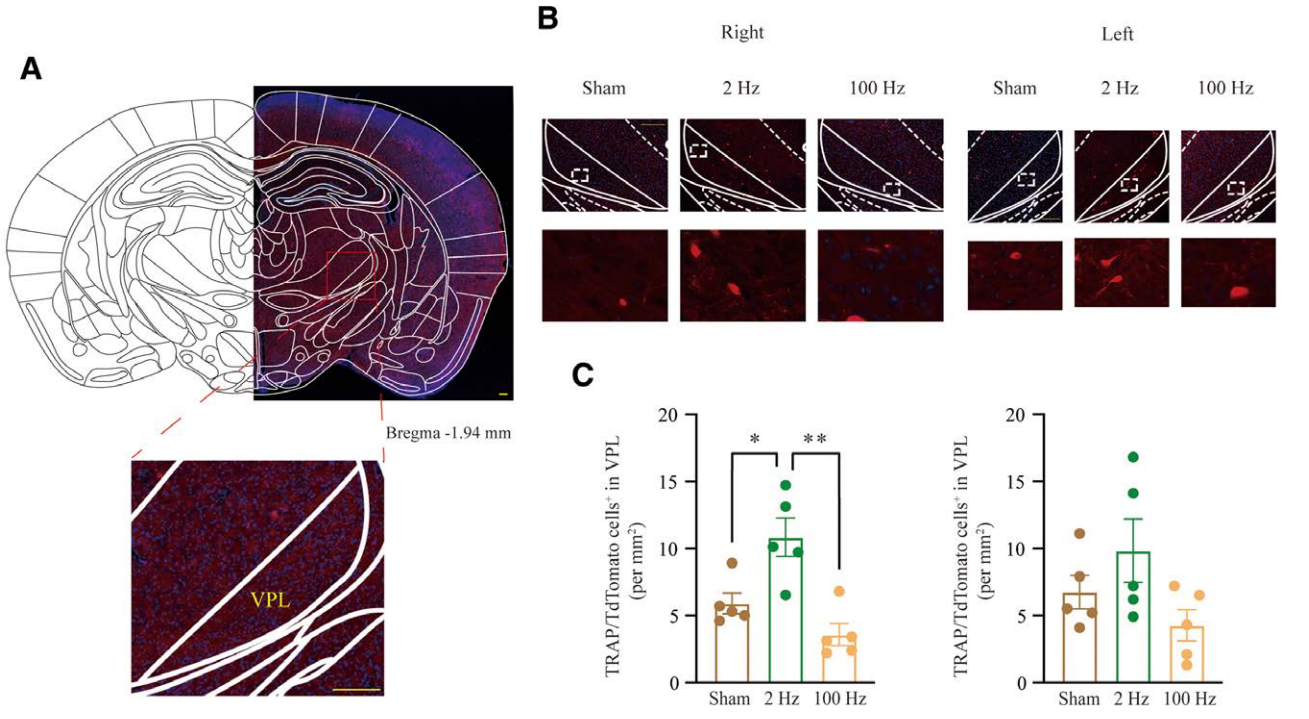

Figure 3. Higher activation of VPL in the thalamus by 2 Hz EA. (A) A representative figure showing the location of VPL. (B) Representative images of EA-TRAPed cells in the bilateral VPL in the different groups of mice, the scare bar: 200 μm. (C) In the VPL, the number of TRAPed cells activated by EA at 2 Hz on the right side was significantly higher than at sham and 100 Hz, data are presented as mean ± SEM on the right, $F_{2,12} = 12.33$, $P = 1.0012$, *post hoc* Tukey test: $^{**}P = 0.0010$ (2 *vs*. 100 Hz), $^{*}P = 0.0161$(sham *vs*. 2 Hz), $P = 0.3003$ (sham *vs*. 100 Hz); on the left, $F_{2,12} = 2.746$, $P = 0.1043$, *post hoc* Tukey test: $P = 0.0883$ (2 *vs*. 100 Hz), $P = 0.4240$ (sham *vs*. 2 Hz), $P = 0.5652$ (sham *vs*. 100 Hz), $n = 5$, $^{*}P < 0.05$, $^{**}P < 0.01$ compared with 2 Hz. EA: Electroacupuncture; SEM: Standard error of the mean; VPL: Ventral posterolateral thalamic nucleus.

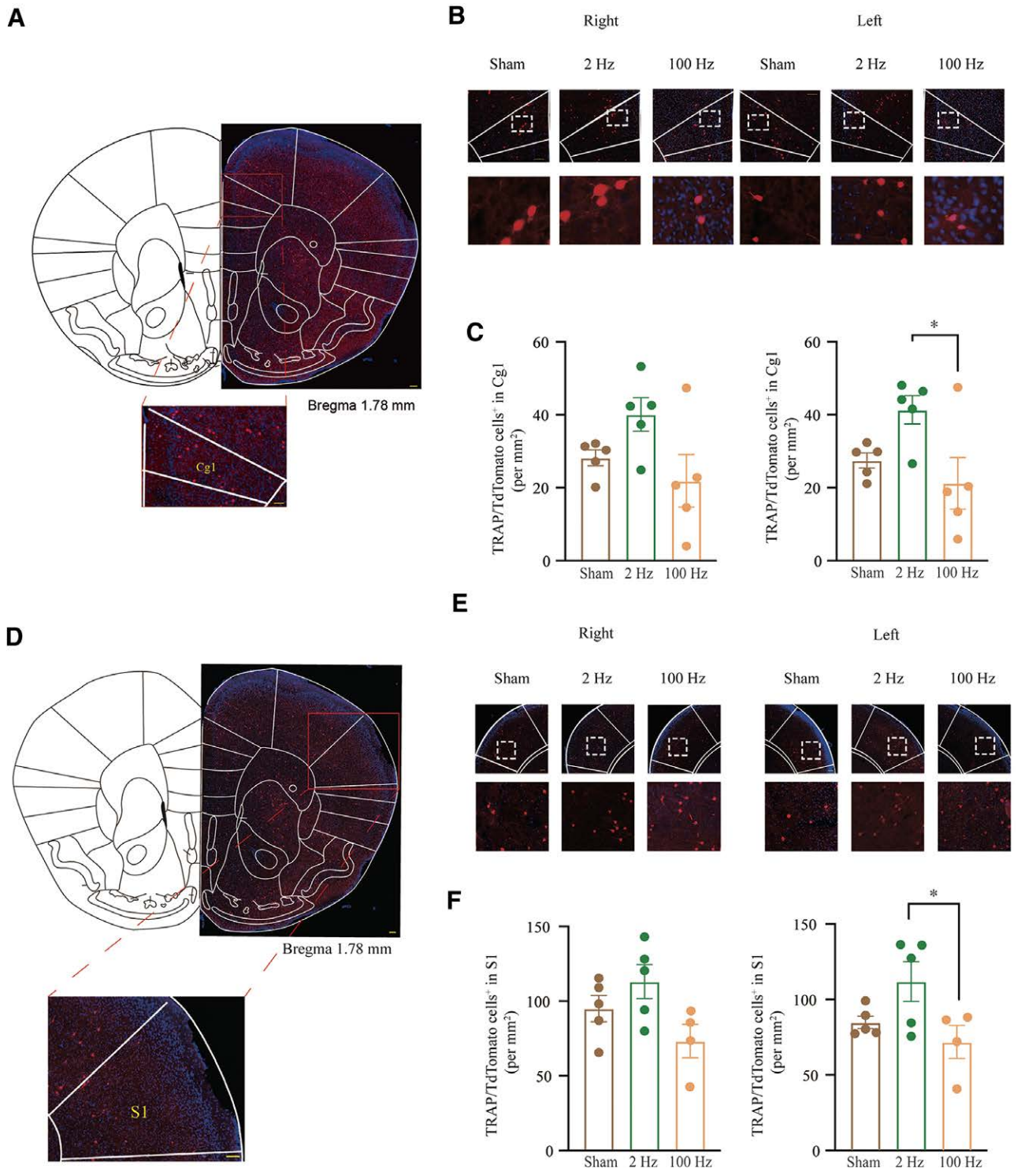

Figure 4. Higher activation of Cg1, S1 in the thalamus by 2 Hz EA. (A) A representative figure showing the location of Cg1. (B) Representative images of EA-TRAPed cells in the bilateral Cg1 in the different groups of mice, the scare bar: 200 μm. (C) In the Cg1, the number of TRAPed cells activated by EA at 2 Hz on the left side was significantly higher than at 100 Hz, data are presented as mean ± SEM, on the right, $F_{2,12} = 3.325$, $P = 0.0710$, *post hoc* Tukey test: $P = 0.0626$ (2 *vs*. 100 Hz), $P = 0.2604$ (sham *vs*. 2 Hz), $P = 0.6620$ (sham *vs*. 100 Hz); on the left, $F_{2,12} = 4.606$, $P = 0.0328$, *post hoc* Tukey test: $^*P = 0.0295$ (2 *vs*. 100 Hz), $P = 0.1441$ (sham *vs*. 2 Hz), $P = 0.6377$ (sham *vs*. 100 Hz), $n = 5$. (D) A representative figure showing the location of S1. (E) Representative images of EA-TRAPed cells in the bilateral S1 in the different groups of mice, the scare bar: 200 μm. (F) In the S1, the number of TRAPed cells activated by EA at 2 Hz on the left side was significantly higher than at 100 Hz, data are presented as mean ± SEM, on the right, $F_{2,11} = 3.425$, $P = 0.0698$, *post hoc* Tukey test: $P = 0.0576$ (2 *vs*. 100 Hz), $P = 0.4461$ (sham *vs*. 2 Hz), $P = 0.3595$ (sham *vs*. 100 Hz); on the left, $F_{2,11} = 3.996$, $P = 0.0496$, *post hoc* Tukey test: $^*P = 0.0481$ (2 *vs*. 100 Hz), $P = 0.1703$ (sham *vs*. 2 Hz), $P = 0.6619$ (sham *vs* 100 Hz), $n = 4$–5, $^*P < 0.05$, compared with 2 Hz. Cg1: Cingulate cortex area 1; EA: Electroacupuncture; S1: Primary somatosensory cortex; SEM: Standard error of the mean.

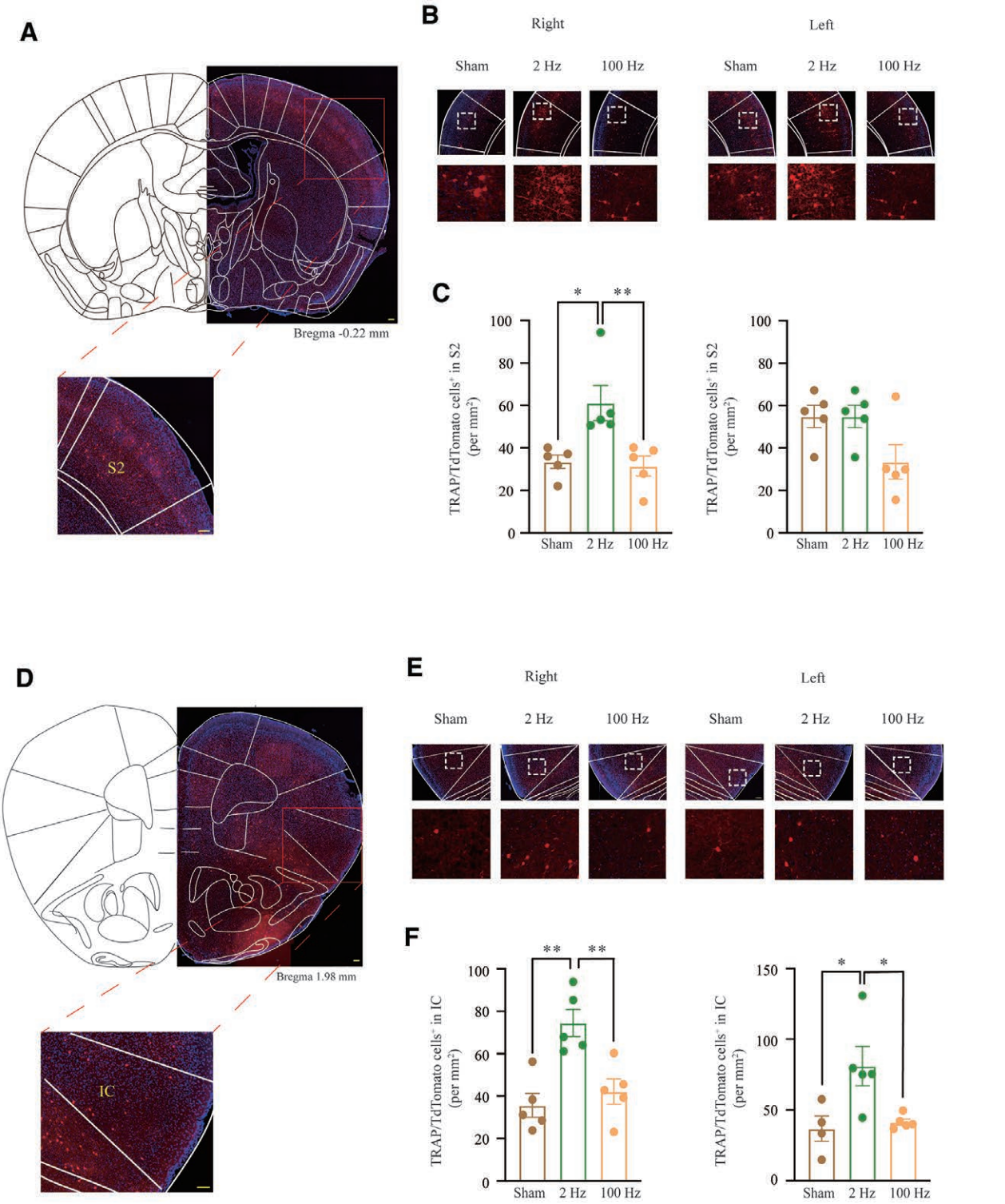

Figure 5. Higher activation of S2, IC in the thalamus by 2 Hz EA. (A) A representative figure showing the location of S2. (B) Representative images of EA-TRAPed cells in the bilateral S2 in the different groups of mice, the scare bar: 200 μm. (C) In the S2, the number of TRAPed cells activated by EA at 2 Hz on the right side was significantly higher than at sham, the number of TRAPed cells activated by EA at 2 Hz on the right side was significantly higher than at 100 Hz, data are presented as mean ± SEM, on the right, $F_{2,12} = 8.138$, $P = 0.0058$, *post hoc* Tukey test: $^{**}P = 0.0093$ (2 *vs*. 100 Hz), $^{*}P = 0.0143$ (sham *vs*. 2 Hz), $P = 0.9687$ (sham *vs*. 100 Hz); on the left, $F_{2,12} = 3.745$, $P = 0.0545$, *post hoc* Tukey test: $P = 0.0838$ (2 *vs*. 100 Hz), $P > 0.9999$ (sham *vs*. 2 Hz), $P = 0.0838$, $n = 5$. (D) A representative figure showing the location of IC. (E) Representative images of EA-TRAPed cells in the bilateral IC in the different groups of mice, the scare bar: 200 μm. (F) In the IC, the number of TRAPed cells activated by EA at 2 Hz on both sides was significantly higher than at sham, the number of TRAPed cells activated by EA at 2 Hz on both sides was significantly higher than at 100 Hz, data are presented as mean ± SEM, on the right, $F_{2,12} = 11.89$, $P = 0.0014$, *post hoc* Tukey test: $^{**}P = 0.0068$ (2 *vs*. 100 Hz), $^{**}P = 0.0018$ (sham *vs*. 2 Hz), $P = 0.7278$ (sham *vs*. 100 Hz); on the left, $F_{2,11} = 6.312$, $P = 0.0149$, *post hoc* Tukey test: $^{*}P = 0.0318$ (2 *vs*. 100 Hz), $^{*}P = 0.0242$ (sham *vs*. 2 Hz), $P = 0.9430$ (sham *vs.* 100 Hz), $n = 3$, $^{*}P < 0.05$, $^{**}P < 0.01$ compared with 2 Hz. EA: Electroacupuncture; IC: Insular cortex; S2: Secondary somatosensory cortex; SEM: Standard error of the mean.

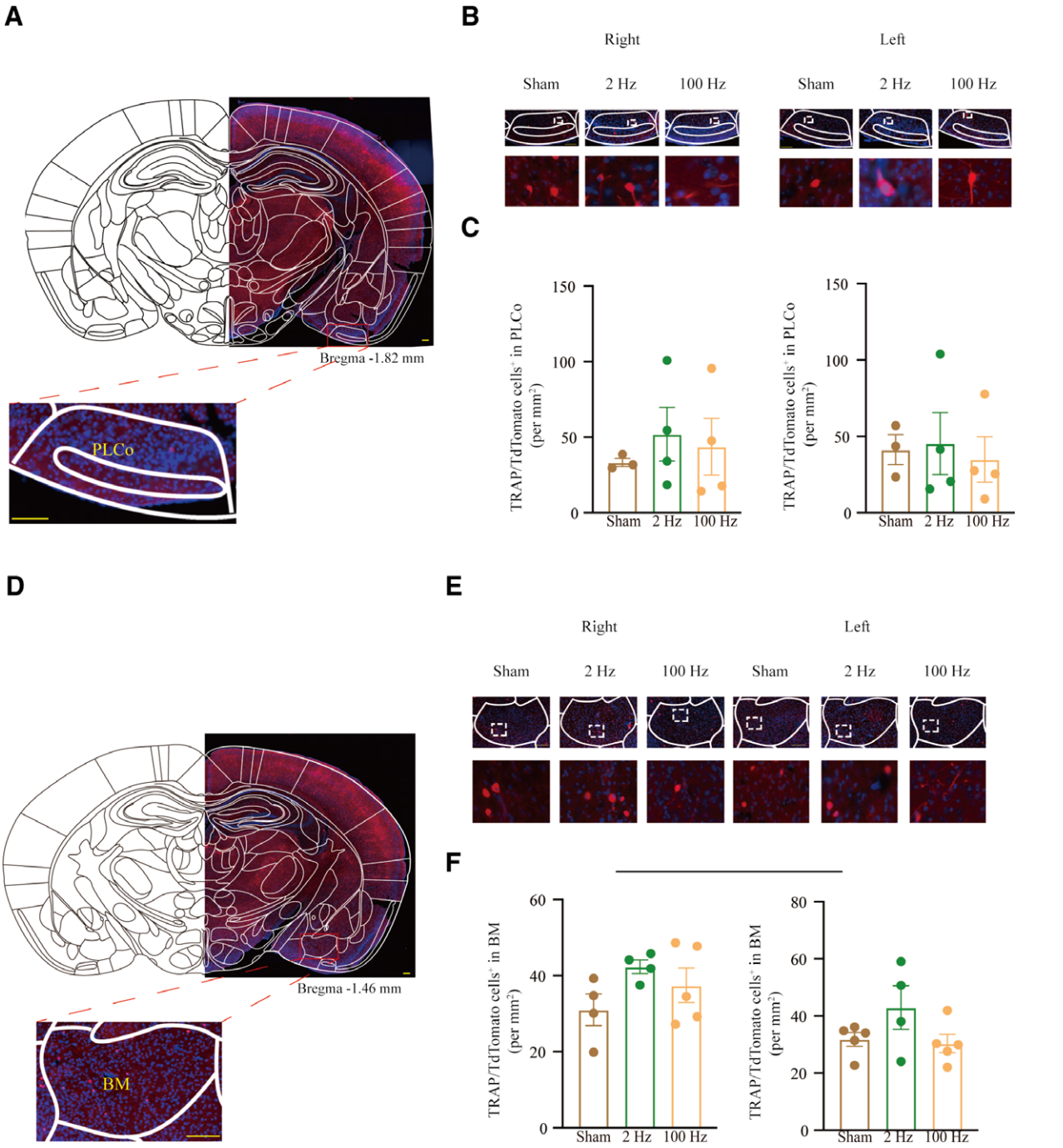

Figure 6. The activation level of PLCo and BM in the amygdala at different frequencies. (A) A representative figure showing the location of PLCo. (B) Representative images of EA-TRAPed cells in the bilateral PLCo in the different groups of mice, the scare bar: 200 μm. (C) In the PLCo, no significant difference between the three groups, data are presented as mean ± SEM, on the right, $F_{2,8} = 0.2927$, $P = 0.7539$, *post hoc* Tukey test: $P = 0.9305$ (2 *vs*. 100 Hz), $P = 0.7335$ (sham *vs*. 2 Hz), $P = 0.9048$ (sham *vs*. 100 Hz); on the left, $F_{2,8} = 0.1096$, $P = 0.8975$, *post hoc* Tukey test: $P = 0.8893$ (2 *vs*. 100 Hz), $P = 0.9851$ (sham *vs*. 2 Hz), $P = 0.9622$ (sham *vs*. 100 Hz), $n = 3$–4. (D) A representative figure showing the location of BM. (E) Representative images of EA-TRAPed cells in the bilateral BM in the different groups of mice, the scare bar: 200 μm. (F) In the BM, no significant difference between the three groups, on the right, data are presented as mean ± SEM, $F_{2,10} = 1.956$, $P = 0.1918$, *post hoc* Tukey test: $P = 0.6535$ (2 *vs*. 100 Hz), $P = 0.1698$ (sham *vs*. 2 Hz), $P = 0.4908$ (sham *vs*. 100 Hz); on the left, $F_{2,11} = 2.178$, $P = 0.1596$, *post hoc* Tukey test: $P = 0.1733$ (2 *vs*. 100 Hz), $P = 0.2428$ (sham *vs*. 2 Hz), $P = 0.9691$ (sham *vs*. 100 Hz), $n = 4$–5. BM: Basomedial amygdaloid nucleus; EA: Electroacupuncture; PLCo: Posterolateral cortical amygdaloid nucleus; SEM: Standard error of the mean.

Activation of hypothalamus nuclei by EA at different frequencies

As for the hypothalamus, we examined three regions: the dorsomedial hypothalamic nucleus (DM), paraventricular hypothalamic nucleus (Pa), and ventromedial hypothalamic nucleus (VMH).

No significant difference in the number of the TRAPed neurons was observed among the sham, 2 Hz, and 100 Hz groups in bilateral DM, Pa, VMH, with measurements were taken at different coordinates along the bregma axis ranging from –1.34 to –2.18, -0.58 to -1.22, -1.06 to -2.06 respectively [Figure 7A–F, Supplementary Figure S10, http://links.lww.com/AHM/A108].

Discussion

The goal of EA is to control bodily functions through acupuncture points[44–47], and the distinctiveness of each

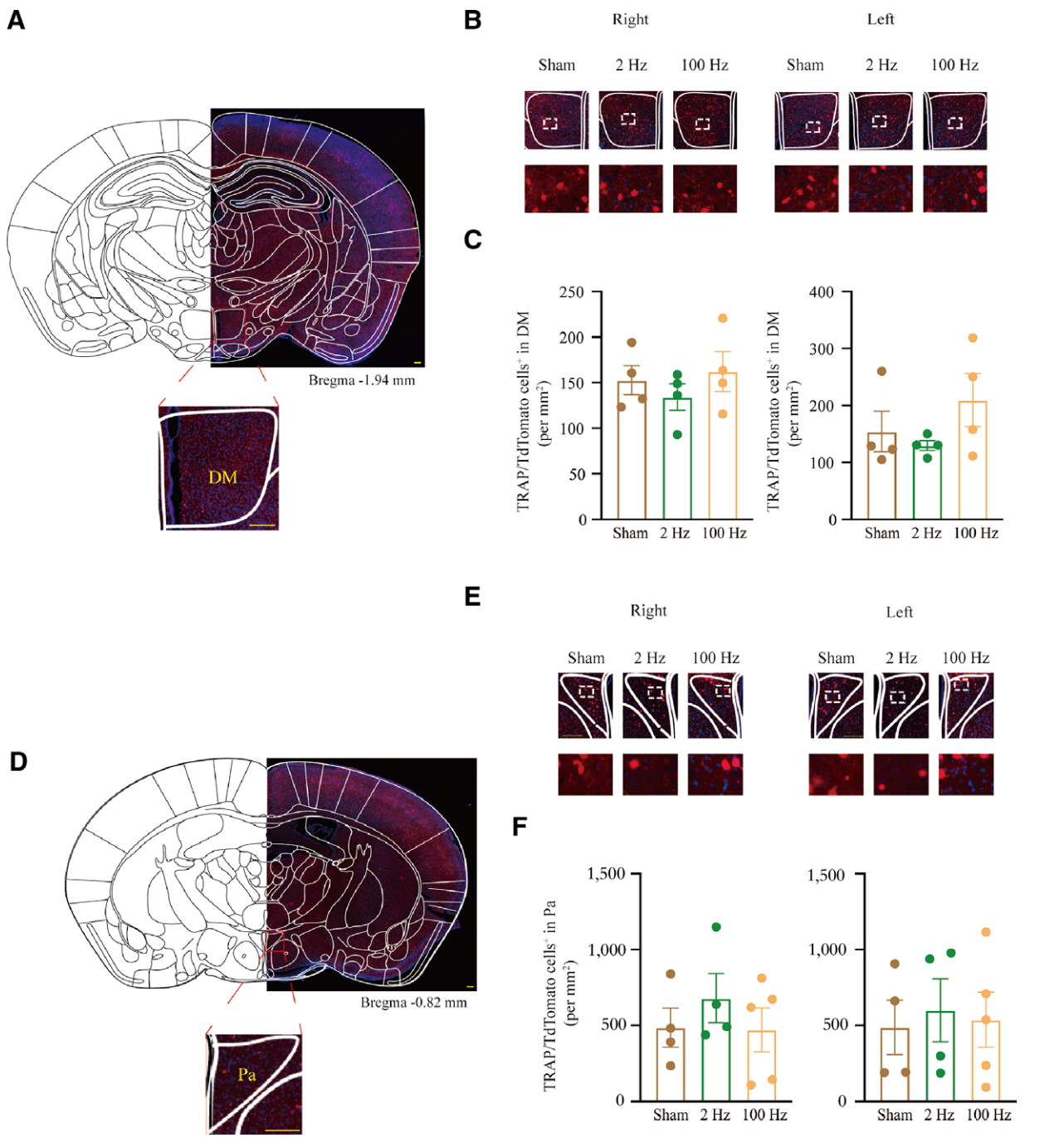

Figure 7. The activation level of DM and Pa in the hypothalamic at different frequencies. (A) A representative figure showing the location of DM. (B) Representative images of EA-TRAPed cells in the bilateral DM in the different groups of mice, the scare bar: 200 μm. (C) In the DM, no significant difference between the three groups, data are presented as mean ± SEM, on the right, $F_{2,9}$ = 0.6417, P = 0.5489, *post hoc* Tukey test: P = 0.5293 (2 *vs*. 100 Hz), P = 0.7515 (sham *vs*. 2 Hz), P = 0.9230 (sham *vs*. 100 Hz); on the left, $F_{2,9}$ = 1.436, P = 0.2876, *post hoc* Tukey test: P = 0.2737 (2 *vs*. 100 Hz), P = 0.8682 (sham *vs*. 2 Hz), P = 0.5129 (sham *vs*. 100 Hz), n = 4. (D) A representative figure showing the location of Pa. (E) Representative images of EA-TRAPed cells in the bilateral Pa in the different groups of mice, the scare bar: 200 μm. (F) In the Pa, no significant difference between the three groups, data are presented as mean ± SEM, on the right, $F_{2,10}$ = 0.6083, P = 0.5632, *post hoc* Tukey test: P = 0.5832 (2 *vs*. 100 Hz), P = 0.6549 (sham *vs*. 2 Hz), P = 0.9969 (sham *vs* 100 Hz); on the left, $F_{2,10}$ = 0.08173, P = 0.9221, *post hoc* Tukey test: $F_{2,10}$ = 0.08173, P = 0.9221, *post hoc* Tukey test: P = 0.9704 (2 *vs*. 100 Hz), P = 0.9149 (sham *vs*. 2 Hz), P = 0.9800 (sham *vs*. 100 Hz), n = 4–5. DM: Dorsomedial hypothalamic nucleus; EA: Electroacupuncture; Pa: Paraventricular hypothalamic nucleus; SEM: Standard error of the mean.

acupoint's local anatomical structure defines how this method works[48,49]. The ST36 point on the lateral edge of the calf is the Xiahe point on the Foot-Yangming's stomach meridian[50]. ST36 is the most frequently used acupoint for analgesia and the most frequently chosen acupoint in acupuncture therapy[51–53]. A study by Harvard University's Ma Qiufu team revealed that EA ST36 can activate the anti-inflammatory pathway of the vagal–adrenal axis. PROKR2 cell activation is enriched in the deep layer of the ST36 acupoint area. When PROKR2 nerve cells were downregulated in the ST36 acupoint area by optogenetic stimulation, analgesic and anti-inflammatory actions essentially disappeared[54]. This finding supports the use of acupuncture as a pain relief agent.

To determine the therapeutic effect of different frequencies of EA on a variety of pains, we chose a low-frequency

EA group with a parameter of 2 Hz and a high-frequency EA group with a parameter of 100 Hz for comparison. Clinical research has demonstrated the clinical efficacy of EA for a range of pain frequencies. Senile postherpetic neuralgia can be treated with EA on the Jiaji point (EX-B2) with moxibustion on the Ashi point; compared with high-frequency EA, low-frequency EA is more efficient[55]. Based on oral pregabalin use, additional EA therapy can relieve anxiety, depression, and can improve sleep quality in patients with postherpetic neuralgia. EA with a 2/100 Hz sparse-dense wave has more significant effects on pain and anxiety reduction than those of EA with a 2 Hz continuous wave[56]. Fundamental research has revealed the mechanisms of high- and low-frequency EA during analgesia. In comparison to high-frequency EA, low-frequency EA enhances the level of c-Fos expression in the arcuate nucleus (Arc)[21]. In a rat slow transit constipation model, EA at ST36 was able to lessen the colon pathology and enhance the morphology of the interstitial cells of Cajal. The treatment decreased the expression of PINK1, Parkin, Beclin1, and LC3 protein at the gene level, but increased the expression of c-Kit and p62 protein, especially for high-frequency EA[57]. The mice's depressive-like behavior and cognitive abilities can be partially improved by EA at 2, 15, and 100 Hz[58]. We found that although both 2 and 100 Hz were capable of treating pain, such as inflammatory pain and neuropathic pain[3,59], 2 Hz EA is better at treating neuropathic pain and 100 Hz EA is more suitable for treating inflammatory pain[60]. To target the clinical treatment of inflammatory and neuropathic pain by high- and low-frequency EA more precisely, we focused on evaluating potential variations in the number of neuronal cells in the brain regions between high- and low-frequency EA. Relying on the expression of Fos^+ neurons in a whole-brain screening of EA-TRAPed neurons, we found that Cg1, S1, S2, and IC in the cortex and PV, VL, and VPL in the thalamus exhibited altered neuronal excitability levels. Compared with high-frequency EA or sham EA, low-frequency EA demonstrated an upregulation of excitability.

These brain regions have also received attention in earlier studies, the cortex is a key brain region encoding information about acute and chronic pain and negative emotions. In recent years, many researchers have revealed the relationship between Cg1, S1, S2, and IC in the cortex and neuropathic pain, inflammatory pain, cancer pain, as well as pain-induced negative emotions[61–66]. Cg1 is one of the key nuclei for pain sensation and negative emotions[67–69]. It is a widespread recipient of inputs from the thalamus and can directly modulate descending nociceptive inhibition, such as the periaqueductal grey matter of the midbrain. Low-frequency EA inhibits inflammatory pain by downregulating the level of CaMKII-Glu A1 phosphorylation, p-CaMKII, as well as the pCaMKII-PICK1 complex involved in EA analgesia[70]. Our team discovered that EA reduced negative feelings and chronic inflammatory pain by upregulating parvalbumin (PV) but not somatostatin (SOM) in the Cg1[28]. Aminobutyric acid receptor type A (GABAA) and aminobutyric acid receptor type A (GABAB) receptors mediated EA relief of neuropathic pain in rats and the spinal GABA receptors were involved in EA analgesia[71]. Formalin-induced chronic pain in mice showed upregulated activation of calcium signals in the S1 brain region, and 26.3% of primary sensory cortex neurons were activated by both pain and itch[72]. EA relieved neuropathic pain in mice by reversing the upregulation of haptoglobin in S1[27]. Neuronal ensembles in the mouse IC activated during distinct inflammatory conditions can retrieve or suppress associated peripheral immunological responses[73]. Clinical studies have found that the local brain activity of the left IC and its functional network with the sensorimotor, cognitive, and executive brain functions in the resting state of patients with asthma are abnormal, and that EA can modulate the functional connectivity of the left insula with the sensorimotor and default networks to alleviate[74]. GABAergic CeA neurons project to glutamatergic parafascicular thalamus (PF) neurons, which project to neurons in S2, and inhibition of this loop alleviates the comorbidity of pain and depression[75].

The thalamus receives projections from many ascending pain pathways and the somatosensory cortex receives information from the thalamocortical pathway[76]. The thalamus consists of the major, medial dorsal, and anterior nuclei. The VP, which consists of the VPL and VPM, has recently been recognized as a crucial brain area for the control of pain and unpleasant emotions. The VPL, the primary somatosensory nucleus of the thalamus, receives and integrates pain information while separating its affective and sensory components[77]; Chronic pain is reduced by HCN2 channel dysfunction and activation in the VPLGlu-S1HLGlu thalamocortical circuit. Remifentanil produces postoperative hyperalgesia by increasing T-type calcium channel-dependent burst firing in VPL Glu neurons to activate S1HLGlu neurons[78], whereas low-frequency EA reduces remifentanil-induced hyperalgesia by lowering the excitability of the VPL neurons[79]. Similarly, the EA-TRAPed neurons were counted in the whole brain, which were found to be directly activated by EA, consistent with the previously reported finding that the activation level of low-frequency EA is upregulated compared with others. This could be connected to our group's findings that low-frequency EA works better for treating neuropathic pain. The relationship between the high activation level of low-frequency EA for Cg1, S1, S2, IC, VPL, VL, and PV and the effectiveness of the treatment of neuropathic pain needs to be explored in future experiments to provide a more thorough justification for the variations in clinical indications guided by EA at different frequencies.

It is well known that the physiological characteristics of the left and right brain are different[80]. The left brain is mainly engaged in logical thinking, whereas the right brain is mainly engaged in figurative thinking, acting as the source of creativity and the center of artistic and experiential learning. The development of brain potential focuses on the development of the right brain. The left brain is the "native brain," which records the knowledge of human beings since birth and manages recent and immediate information. The right brain is the potential stimulation area, and suddenly shows signs in the deeper layers of spiritual life. It is the area of explosive creativity, and it not only has the magical ability to

memorize but also has the ability to process information at high speed. A developed right brain may suddenly be struck with a kind of fantasy, a piece of innovation, and an invention, etc. The right brain is a low-consumption and high-efficiency working area, which does not need a lot of energy to perform high-speed calculation of complex mathematical problems, high-speed memory, high-quality memory, with the ability to forget. A lot of emotional behavior is also controlled by the right brain[81]. Due to the different physiological functions of the left and right brain, responses to EA stimulation is different. It is plausible that EA activates the left and right brain differently because of the aforementioned variations in physiological features.

The FosCreER system is used to clarify how neurons are activated by different frequencies of EA, and to investigate the differences between the activation levels of high-frequency and low-frequency EA in brain regions. We established a genetic method to visualize EA-activated neurons. The differences between high- and low-frequency EA were demonstrated at the level of neurons, and the findings of the study indicated that different brain regions have different EA activation levels. These findings have laid the groundwork for the use of EA in the treatment of clinical disorders (Figure 8).

This study has several limitations. First, there are many factors affecting the therapeutic effect of EA, such as intensity, treatment time, and acupoints; however, this experiment only demonstrated the effect of different frequencies of EA on the degree of activation of brain areas. Second, EA activates some nuclei; however, whether EA analgesia is related to the activation of these nuclei needs to be explored. Third, the mechanism by which EA activates these nuclei and whether it is mediated by certain substances have not been explored.

Conclusion

Based on the above results, both high- and low-frequency EA, as well as sham EA, can directly activate brain regions. Low-frequency EA resulted in better activation of the VPL, VL, and PV in the thalamus, as well as Cg1, S1, S2, and IC in the cortex, suggesting that the frequency of EA may be a crucial parameter in EA treatment.

Conflict of interest statement

The authors declare no conflict of interest.

Funding

This work was supported by the National Natural Science Fund of China (82374561, 82174490, 81873360), the Zhejiang Medical and Health Science and Technology Program (2021RC098), the Research Project of Zhejiang Chinese Medical University (2022JKZKTS44).

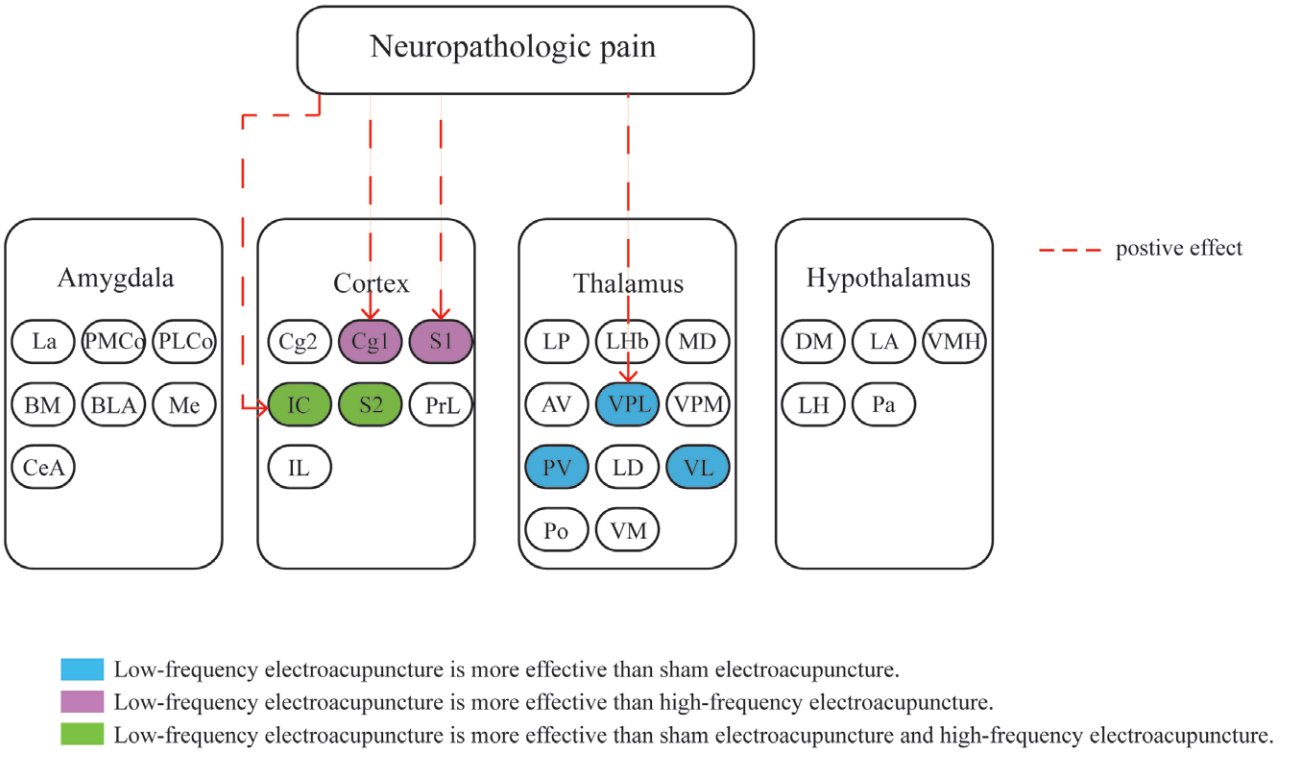

Figure 8. Activation levels of brain regions by EA and correlation with neuropathologic pain. AV: Anteroventral thalamic nucleus; BLA: Basolateral amygdaloid nucleus; BM: Basomedial amygdaloid nucleus; CeA: Central amygdaloid nucleus; Cg1: Cingulate cortex area 1; Cg2: Cingulate cortex area 2; DM: Dorsomedial hypothalamic nucleus; EA: Electroacupuncture; IC: Insular cortex; IL: Infralimbic cortex; LA: Lateral amygdaloid nucleus; LD: Laterodorsal thalamic nucleus; LHb: Lateral habenular nucleus; LP: Lateral posterior thalamic nucleus; MD: Mediodorsal thalamic nucleus; Me: Medial amygdaloid nucleus; Pa: Paraventricular hypothalamic nucleus; PLCo: Posterolateral cortical amygdaloid nucleus; PMCo: Posteromedial cortical amygdaloid nucleus; Po: Posterior thalamic nuclear group; PrL: Prelimbic cortex; PV: Paraventricular thalamic nucleus; S1: Primary somatosensory cortex; S2: Secondary somatosensory cortex; VL: Ventrolateral thalamic nucleus; VM: Ventromedial hypothalamic nucleus; VMH: Ventromedial hypothalamic nucleus; VPL: Ventral posterolateral thalamic nucleus; VPM: Ventral posteromedial thalamic nucleus.

Author contributions

Jianqiao Fang, Junfang Fang, and Junying Du designed the study. Zi Guo, Tiancheng Sun, and Naixuan Wei performed the experiment and wrote the article. Ru Ye, Xiaochang Ge, and Lu Guan participated in analyzing the results. Xiaomei Shao and Shuang Qiu reviewed the text after conducting data analysis. The final manuscript was read and approved by all writers.

Ethical approval of studies and informed consent

All mice experimental were approved by the Animal Care of Zhejiang Chinese Medical Animal Care and Welfare Committee of Zhejiang China (IACUC-20200302-06).

Acknowledgments

We appreciate the technical support from the Public Platform of Medical Research Center, Academy of Chinese Medical Science, Zhejiang Chinese Medical University.

Data availability

All data generated or analyzed during this study are included in this published article.

References

[1] Liu K, Zhu B. Significance of pleasant touch and state-of-the-art neuroscience technologies in acupuncture research. *Acupunct Herb Med* 2023;3(1):55–58.
[2] Acar HV. Acupuncture and related techniques during perioperative period: a literature review. *Complement Ther Med* 2016;29:48–55.
[3] Shen Z, Zhang H, Wu Z, et al. Electroacupuncture alleviates chronic pain-induced anxiety disorders by regulating the rACC-thalamus circuitry. *Front Neurosci* 2021;14:615395.
[4] Vickers AJ, Vertosick EA, Lewith G, et al. Acupuncture for Chronic Pain: Update of an Individual Patient Data Meta-Analysis. *J Pain* 2018;19(5):455-474.
[5] Lee SH, Lee BC. Use of acupuncture as a treatment method for chronic prostatitis/chronic pelvic pain syndromes. *Curr Urol Rep* 2011;12(4):288-96.
[6] Wang L, Hu X, Geng L, et al. Multi-effective characteristics and advantages of acupuncture in COVID-19 treatment. *Acupunct Herb Med* 2023;3(2):83–95.
[7] Li PS, Peng XM, Niu XX, et al. Efficacy of acupuncture for endometriosis-associated pain: a multicenter randomized single-blind placebo-controlled trial. *Fertil Steril* 2023;119(5):815-823.
[8] Wang X, Li JL, Wei XY, et al. Psychological and neurological predictors of acupuncture effect in patients with chronic pain: a randomized controlled neuroimaging trial. *Pain* 2023;164(7):1578-1592.
[9] Zhang X, Qiu H, Li C, et al. The positive role of traditional Chinese medicine as an adjunctive therapy for cancer. *Biosci Trends* 2021;15(5):283–298.
[10] Wei TH, Hsieh CL. Effect of acupuncture on the p38 signaling pathway in several nervous system diseases: a systematic review. *Int J Mol Sci* 2020;21(13):4693.
[11] Kim G, Kim D, Moon H, et al. Acupuncture and Acupoints for Low Back Pain: Systematic Review and Meta-Analysis. *Am J Chin Med* 2023;51(2):223-247.
[12] Kaptchuk TJ. Acupuncture: theory, efficacy, and practice. *Ann Intern Med* 2002;136(5):374-83.
[13] Zhang RX, Lao LX, Ren K, et al. Mechanisms of acupuncture-electroacupuncture on persistent pain. *Anesthesiology* 2014;120(2):482–503.
[14] Oh JE, Kim SN. Anti-inflammatory effects of acupuncture at ST36 point: a literature review in animal studies. *Front Immunol* 2022;12:813748.
[15] Zhang J, Liu Y, Li Z, et al. Functional magnetic resonance imaging studies of acupuncture at ST36: a coordinate-based meta-analysis. *Front Neurosci* 2023;17:1180434.
[16] Kim JH, Kim HK, Park YI, et al. Moxibustion at ST36 alleviates pain in complete Freund's adjuvant-induced arthritic rats. *Am J Chin Med* 2006;34(1):57–67.
[17] Atalay SG, Durmus A, Gezginaslan O. The effect of acupuncture and physiotherapy on patients with knee osteoarthritis: a randomized controlled study. *Pain Physician* 2021;24(3):E269–E278.
[18] Wu SY, Lin CH, Chang NJ, et al. Combined effect of laser acupuncture and electroacupuncture in knee osteoarthritis patients: a protocol for a randomized controlled trial. *Medicine (Baltimore)* 2020;99(12):e19541.
[19] Zhan SQ, Zhao Q, Guo X, et al. Effects of needling Zusanli with. electroacupuncture on the express of intracerebral c-fos of rats. *J Shandong Univ TCM* 2005;1:57–58.
[20] Silva ML, Silva JRT, Prado WA. Analgesia induced by 2- or 100-Hz electroacupuncture in the rat tail-flick test depends on the anterior pretectal nucleus. *Life Sci* 2013;93(20):742–754.
[21] Wang K, Zhang R, He F, et al. Electroacupuncture frequency-related transcriptional response in rat arcuate nucleus revealed region-distinctive changes in response to low and high-frequency electroacupuncture. *J Neurosci Res* 2012;90(7):1464–1473.
[22] Ali U, Apryani E, Wu HY, et al. Low frequency electroacupuncture alleviates neuropathic pain by activation of spinal microglial IL-10/β-endorphin pathway. *Biomed Pharmacother* 2020;125:109898.
[23] Zhou W, Lei R, Zuo C, et al. Analgesic effect of moxibustion with different temperature on inflammatory and neuropathic pain mice: a comparative study. *Evid Based Complement Alternat Med* 2017;2017:4373182.
[24] Guo Z, Lin X, Samaniego T, et al. Fos-CreER-based genetic mapping of forebrain regions activated by acupuncture. *J Comp Neurol* 2020;528(6):953–971.
[25] Bian WJ, Brewer CL, Kauer JA, et al. Adolescent sleep shapes social novelty preference in mice. *Nat Neurosci* 2022;25(7):912–923.
[26] Lin X, Itoga CA, Taha S, et al. c-Fos mapping of brain regions activated by multi-modal and electric foot shock stress. *Neurobiol Stress* 2018;8:92–102.
[27] Ping XJ, Xie JK, Yuan CL, et al. Electroacupuncture induces bilateral S1 and ACC epigenetic regulation of genes in a mouse model of neuropathic pain. *Biomedicines* 2023;11(4):1030.
[28] Shao FB, Fang FB, Qiu MT, et al. Electroacupuncture ameliorates chronic inflammatory pain-related anxiety by activating PV interneurons in the anterior cingulate cortex. *Front Neurosci* 2021;15:691931.
[29] Yuan QL, Wang P, Liu L, et al. Acupuncture for musculoskeletal pain: A meta-analysis and meta-regression of sham-controlled randomized clinical trials. *Sci Rep* 2016;29(6):30675.
[30] Ge WQ, Zhan-Mu OY, Chen C, et al. Electroacupuncture reduces chronic itch via cannabinoid CB1 receptors in the ventrolateral periaqueductal gray. *Front Pharmacol* 2022;13:931600.
[31] Wu ZM, Wang JL, Xu LL, et al. Effects of electroacupuncture on sensory and affective regulation and p-ERK expression in anterior cingulate cortex and somatosensory cortex in CFA rats. *World Chin Med* 2019;14(6):1354–1362.
[32] Link W, Konietzko U, Kauselmann G, et al. Somatodendritic expression of an immediate early gene is regulated by synaptic activity. *Proc Natl Acad Sci USA* 1995;92(12):5734–5738.
[33] Koya E, Golden SA, Harvey BK, et al. Targeted disruption of cocaine-activated nucleus accumbens neurons prevents context-specific sensitization. *Nat Neurosci* 2009;12(8):1069–1073.
[34] Barth AL, Gerkin RC, Dean KL. Alteration of neuronal firing properties after in vivo experience in a FosGFP transgenic mouse. *J Neurosci* 2004;24(29):6466–6475.
[35] Guzowski JF, McNaughton BL, Barnes CA, et al. Environment-specific expression of the immediate-early gene Arc in hippocampal neuronal ensembles. *Nat Neurosci* 1999;2(12):1120–1124.
[36] Garner AR, Rowland DC, Hwang SY, et al. Generation of a synthetic memory trace. *Science* 2012;335(6075):1513–1516.
[37] Corbacho J, Sanabria-Reinoso E, Buono L, et al. Trap-TRAP, a versatile tool for tissue-specific translatomics in zebrafish. *Front Cell Dev Biol* 2022;9:817191.
[38] Liu J, Totty MS, Melissari L, et al. Convergent coding of recent and remote fear memory in the basolateral amygdala. *Biol Psychiatry* 2022;91(9):832–840.
[39] Guenthner CJ, Miyamichi K, Yang HH, et al. Permanent genetic access to transiently active neurons via TRAP: targeted recombination in active populations. *Neuron* 2013;78(5):773–784.
[40] Cho E, Kim W. Effect of acupuncture on diabetic neuropathy: a narrative review. *Int J Mol Sci* 2021;22(16):8575.
[41] Kolev HM, Tian Y, Kim MS, et al. A FoxL1-CreERT-2AtdTomato mouse labels subepithelial telocytes. *Cell Mol Gastroenterol Hepatol* 2021;12(3):1155–1158.e4.

[42] Wu M, Chen Y, Shen Z, et al. Electroacupuncture alleviates anxiety-like behaviors induced by chronic neuropathic pain via regulating different dopamine receptors of the basolateral amygdala. *Mol Neurobiol* 2022;59(9):5299–5311.
[43] Li Y, Yin C, Li X, et al. Electroacupuncture alleviates paclitaxel-induced. peripheral neuropathic pain in rats via suppressing TLR4 signaling and TRPV1 upregulation in sensory neurons. *Int J Mol Sci* 2019;20(23):5917.
[44] MacPherson H, Vertosick EA, Foster NE, et al. Acupuncture Trialists' Collaboration. The persistence of the effects of acupuncture after a course of treatment: a meta-analysis of patients with chronic pain. *Pain* 2017;158(5):784-793.
[45] Wang M, Liu W, Ge J, et al. The immunomodulatory mechanisms for acupuncture practice. *Front Immunol* 2023;14:1147718.
[46] Butt MF, Albusoda A, Farmer AD, et al. The anatomical basis for transcutaneous auricular vagus nerve stimulation. *J Anat* 2020;236(4):588–611.
[47] Chen J, Lin Z, Ding J. Zusanli (ST36) acupoint injection with dexamethasone for chemotherapy-induced myelosuppression: a systematic review and meta-analysis. *Front Oncol* 2021;11:684129.
[48] Zhu B. On the acupoint and its specificity. *Chin Acupunct Moxibustion* 2021;41(9):945–950.
[49] Hall H. Acupuncture's claims punctured: not proven effective for pain, not harmless. *Pain* 2011;152(4):711-712.
[50] Almeida RT, Perez AC, Francischi JN, et al. Opioidergic orofacial antinociception induced by electroacupuncture at acupoint St36. *Braz J Med Biol Res* 2008;41(7):621–626.
[51] Feng Y, Fang Y, Wang Y, et al. Acupoint therapy on diabetes mellitus and its common chronic complications: a review of its mechanisms. *Biomed Res Int* 2018;2018:3128378.
[52] Lai F, Ren Y, Lai C, et al. Acupuncture at Zusanli (ST36) for experimental sepsis: a systematic review. *Evid Based Complement Alternat Med* 2020;2020:3620741.
[53] Zhao P, Fu H, Cheng H, et al. Acupuncture at ST36 alleviates the behavioral disorder of autistic rats by inhibiting TXNIP-mediated activation of NLRP3. *J Neuropathol Exp Neurol* 2022;81(2):127–134.
[54] Liu S, Wang Z, Su Y, et al. A neuroanatomical basis for electroacupuncture to drive the vagal–adrenal axis. *Nature* 2021;598(7882):641–645.
[55] Li DC, Song YT, Ren YJ, et al. Observation on the curative effect of different frequency electro-acupuncture at Jiaji (EXB2) combined with peri-acupuncture at Ashi point and mild moxibustion in the treatment of senile postherpetic neuralgia. *Guiding J Tradit Chin Med Pharm* 2023;29(3):114–118.
[56] Ren LL, Sun RH, Li SM. Efficacy comparison of electroacupuncture with different frequencies combined with Pregabalin for postherpetic neuralgia. *Shanghai J Acu-mox* 2023;42(2):142–146.
[57] Wu ZW, Liu M, Lou YJ, et al. Mechanism of electroacupuncture with different frequencies in the regulation of PINK1/Parkin pathway activity in a rat model of slow transit constipation (STC). *Zhejiang J Integr Tradit Chin West Med* 2023;33(2):106–111.
[58] Xie YY, Liu LS, Chen JD. Influence of different frequency of electroacupuncture on cognitive function of depression-like mice. *Guangming J Chin Med* 2022;37(17):3116–3121.
[59] Xiang X, Wang S, Shao F, et al. Electroacupuncture stimulation alleviates CFA-induced inflammatory pain via suppressing P2X3 expression. *Int J Mol Sci* 2019;20(13):3248.
[60] Fang JQ, Du JY, Fang JF, et al. Parameter-specific analgesic effects of electroacupuncture mediated by degree of regulation TRPV1 and P2X3 in inflammatory pain in rats. *Life Sci* 2018;200:69–80.
[61] Zhou H, Li M, Zhao R, et al. A sleep-active basalocortical pathway crucial for generation and maintenance of chronic pain. *Nat Neurosci* 2023;26(3):458–469.
[62] Smith ML, Asada N, Malenka RC. Anterior cingulate inputs to nucleus accumbens control the social transfer of pain and analgesia. *Science* 2021;371(6525):153–159.
[63] Iqbal Z, Lei Z, Ramkrishnan AS, et al. Adrenergic signalling to astrocytes in anterior cingulate cortex contributes to pain-related aversive memory in rats. *Commun Biol* 2023;6(1):10.
[64] Alonso-Matielo H, Zhang Z, Gambeta E, et al. Inhibitory insula-ACC projections modulate affective but not sensory aspects of neuropathic pain. *Mol Brain* 2023;16(1):64.
[65] Darvish-Ghane S, Baumbach J, Martin LJ. Influence of inflammatory pain and dopamine on synaptic transmission in the mouse ACC. *Int J Mol Sci* 2023;24(13):11113.
[66] Long H, Wang Y, Jian F, et al. Current advances in orthodontic pain. *Int J Oral Sci* 2016;8(2):67–75.
[67] Cao P, Zhang MJ, Ni ZY, et al. Green light induces antinociception via visual-somatosensory circuits. *Cell Rep* 2023;42(4):112290.
[68] Gong JY, Wang JJ, Qiu SJ, et al. Common and distinct patterns of intrinsic brain activity alterations in major depression and bipolar disorder: voxel-based meta-analysis. *Transl Psychiatry* 2020;10(1):353.
[69] Quiroz González S, Segura-Alegría B, Jiménez Estrada I. Depressing effect of electroacupuncture on the spinal non painful sensory input of the rat. *Exp Brain Res* 2014;232(9):2721–2729.
[70] Gu Y, Chen S, Mo Y, et al. Electroacupuncture attenuates CFA-induced inflammatory pain by regulating CaMKII. *Neural Plast* 2020;2020:8861994.
[71] Park JH, Han JB, Kim SK, et al. Spinal GABA receptors mediate the suppressive effect of electroacupuncture on cold allodynia in rats. *Brain Res* 2010;1322:24–29.
[72] Ishikawa T, Murata K, Okuda H, et al. Pain-related neuronal ensembles in the primary somatosensory cortex contribute to hyperalgesia and anxiety. *iScience* 2023;26(4):106332.
[73] Koren T, Yifa R, Amer M, et al. Insular cortex neurons encode and retrieve specific immune responses. *Cell* 2021;184(24):5902–5915.e17.
[74] Chen H, Wei XY, Gong ZG, et al. Study on electroacupuncture regulating the brain function in patients with asthma. *Chin J Med Imag Technol* 2022;20(1):5–10.
[75] Zhu X, Zhou W, Jin Y, et al. A central amygdala input to the parafascicular nucleus controls comorbid pain in depression. *Cell Rep* 2019;29(12):3847–3858.e5.
[76] Jabaudon D, López Bendito G. Development and plasticity of thalamocortical systems. *Eur J Neurosci* 2012;35(10):1522–1523.
[77] Yu JM, Hu R, Mao Y, et al. Up-regulation of HCN2 channels in a thalamocortical circuit mediates allodynia in mice. *Natl Sci Rev* 2022;10(2):nwac275.
[78] Jin Y, Mao Y, Chen D, et al. Thalamocortical circuits drive remifentanil-induced postoperative hyperalgesia. *J Clin Invest* 2022;132(24):e158742.
[79] Zhao HY, Liu LY, Cai J, et al. Electroacupuncture treatment alleviates the remifentanil-induced hyperalgesia by regulating the activities of the ventral posterior lateral nucleus of the thalamus neurons in rats. *Neural Plast* 2018;2018:1–15.
[80] Wan B, Bayrak S, Xu T, et al. Heritability and cross-species comparisons of human cortical functional organization asymmetry. *Elife* 2022;11:e77215.
[81] Liang X, Zhao C, Jin X, et al. Sex-related human brain asymmetry in hemispheric functional gradients. *Neuroimage* 2021;229:117761.